Molecular actuation of a bistable liquid-crystalline [c2]daisy chain rotaxane

Christian C Carmona-Vargas, Lara Faour, Shoichi Tokunaga, Doru Constantin, Guillaume Fleith, Emilie Moulin, Nicolas Giuseppone

RESEARCH ARTICLE

Molecular actuation of a bistable liquid-crystalline [*c*2]daisy chain rotaxane

Christian C. Carmona-Vargas,[a] Lara Faour,[a] Shoichi Tokunaga,[a] Doru Constantin,[b] Guillaume Fleith,[b] Emilie Moulin,[a] and Nicolas Giuseppone*[a,c]

[a] Dr. C. C. Carmona-Vargas, Dr. L. Faour, Dr. S. Tokunaga, Dr. E. Moulin and Prof. Dr. N. Giuseppone
SAMS Research Group Université de Strasbourg, CNRS, Institut Charles Sadron UPR 22 67000 Strasbourg, France
E-mail: giuseppone@unistra.fr

[b] Dr. D. Constantin, G. Fleith
Université de Strasbourg, CNRS, Institut Charles Sadron UPR 22 67000 Strasbourg, France

[c] Institut Universitaire de France (IUF)

Supporting information for this article is given via a link at the end of the document.

Abstract: A bistable [*c*2]daisy chain rotaxane bearing two mesogen units was synthesized, and its liquid crystal phase diagram was characterized. As a remarkable result, we demonstrate that, depending on the contracted or extended state of its mechanical bond, the system can convert between an isotropic and a smectic A mesophase at constant temperature.

Introduction

Artificial molecular machines can generate controlled nanoscale movements by using the precise mechanical actuation of their internal components.[1–5] For instance, molecular machines based on mechanically interlocked molecules (MIMs), such as rotaxanes and catenanes,[6–8] have been implemented across various fields of research, ranging from synthetic organic chemistry[9–11] to materials science.[12–17] Of particular interest, the interlocked topology of [*c*2]daisy chain rotaxanes has been inspired by the sliding movement that takes place inside a sarcomere, the basic contracting unit of our muscles.[18,19] When made bistable, [*c*2]daisy chain rotaxanes can undergo a molecular extension / contraction switching process controlled by external stimuli (*e.g.* pH,[20,21] redox potential,[22] solvent,[23] or light[24,25]).[26,27]

In principle, when coupling many of these tiny MIMs with one another in space and time, their movements can be transferred and amplified from molecular to higher length scales,[28] with the potential to access an infinity of new dynamic and active systems with responsive properties.[15,29–31] A few seminal examples of the amplifications of nanoscopic motions at meso- and macroscale have been recently achieved in polymer and self-assembled soft materials such as physical and chemical gels.[14,32–35] However, the collective actuation of MIMs remains to date much less studied in fluid-oriented materials such as liquid crystals (LCs). This would be of peculiar interest because LC mesophases represent an anisotropic - while dynamic - environment[36–38] that can in principle sense and translate the nanoactuations generated by MIMs.[39–43] In that direction, Sauvage and collaborators reported for the first time in 2007 the formation of a [2]catenane exhibiting a liquid-crystalline behaviour.[40] In parallel, a collaborative work between Kato's and Stoddart's teams led to the first synthesis of a [2]rotaxane displaying LC properties.[41] The formation of a smectic A (SmA) mesophase over a wide range of temperatures (10 – 150 °C) was characterized by combining polarized optical microscopy (POM) and small angle X-ray scattering (SAXS) experiments. Nevertheless, in the aforementioned examples, the interlocked mechanical motions did not modify the corresponding LC phase diagrams.

Now, we report the synthesis and the characterisation of a [*c*2]daisy chain rotaxane decorated with two mesogenic units. By analysing this system at various length scales, we demonstrate that the actuation of the pH-sensitive mechanical bond triggers the contraction and extension of the [*c*2]daisy chain topology, and that such a switching molecular event can consequently shift the LC phase diagram of the material.

Results and Discussion

We chose as mesogen a dendritic structure known to induce liquid crystalline properties[40] and to decrease phase transitions temperatures because of its fluoro-substituents.[44] This dendritic molecule, derived from gallic acid, contains rigid dendrons composed of 2,3-difluoro-4'-(4-pentylcyclohexyl)-biphenyl fragments attached through a flexible spacer based on a triethylene oxide chain to the gallic moiety. Similar structures have been used to induce the formation of liquid crystalline phases when covalently bound to non-mesogenic functional molecules such as catenanes and rotaxanes.[41]

Thus, we designed [*c*2]daisy chain rotaxane **9**, which consists in two main building blocks: pseudo[*c*2]daisy chain rotaxane **7**, and dendritic mesogen **6**. The former was synthesized in 8 steps and 39% overall yield from commercially available 3-octyn-1-ol and catechol, according to previous reports from the literature (see ESI for detailed information).[45,46] For compound, **6**, a Suzuki-Miyaura cross-coupling reaction between commercially available (4-ethoxy-2,3-difluorophenyl)boronic acid and 1-iodo-4-(4-pentylcyclohexyl)benzene,[47] followed by a subsequent classic ether cleavage with boron tribromide afforded compound **1** in high

yields (Scheme 1).[48] Mono-*O*-alkylation of compound **1** using triethyleneglycol di(*p*-toluenesulfonate) led to compound **2**, which was used as alkylating agent for the triple *O*-alkylation of methyl gallate. The resulting methyl ester **3** was subsequently reduced to the corresponding alcohol derivative **4** in very good yield. Then, a chlorination reaction was carried out with compound **4** in the presence of thionyl chloride leading to compound **5**, which was subjected to a nucleophilic substitution with sodium azide to yield mesogen **6** (Scheme 1).

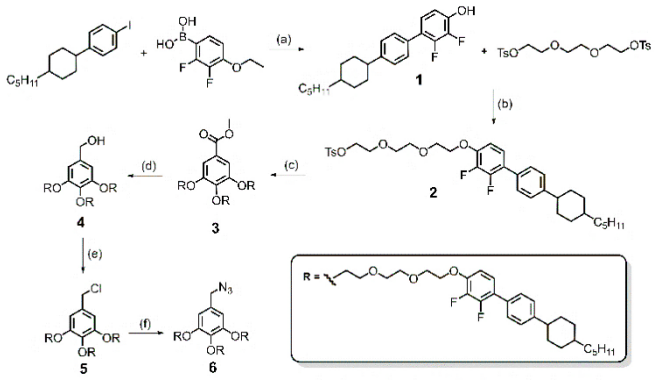

Scheme 1. Synthesis of azide derivative mesogen **6**. *Reagents and conditions*: (a) *i.* $Pd(PPh_3)_4$, K_2CO_3, toluene/ethanol/water, 100 °C, 18h, 84%. *ii.* BBr_3, dry CH_2Cl_2, -78 °C, 2h -> 20 °C, 16h, 96%. (b) K_2CO_3, KI, acetone, 60 °C, 24 h, 70%. (c) methyl gallate, K_2CO_3, 2-butanone, 80 °C, 24 h, 50%. (d) $LiAlH_4$, dry THF, 20 °C, 6 h, 90%. (e) $SOCl_2$, dry CH_2Cl_2, 20 °C, 2 h, 96 %. (f) NaN_3, dry DMF, 90 °C, 24 h, 80 %.

The coupling of mesogen **6** with pseudo[*c*2]daisy chain rotaxane **7** was then achieved by a Copper(I)-catalysed Azide-Alkyne Cycloaddition (CuAAC) "click reaction (Scheme 2).[45,49] Mixing both compounds with an equimolar amount of $Cu(CN)_4PF_6$, 2,6-lutidine under argon atmosphere in dry dichloromethane led, after 3hours of microwave irradiation (40 W), to the formation of [*c*2]daisy chain rotaxane **8** in good yield. Subsequently, compound **8** was subjected to a *N*-methylation reaction of the triazole rings using methyl iodide as solvent under stirring for four days, affording compound **9** in an excellent yield after a liquid-liquid extraction and counterion exchange with a saturated aqueous solution of ammonium hexafluorophosphate (NH_4PF_6).
The reversible molecular actuation of the final [*c*2]daisy chain between its extended state (**9**$_{Ext}$) and its contracted state (**9**$_{Cont}$) was achieved by deprotonation/protonation of the ammonium station using an excess of sodium hydroxide 1 M and of TFA, respectively (see SI). Such actuation was confirmed by recording the ^{1}H NMR spectra of [*c*2]daisy chain **9** in both, extended and contracted states, exhibiting all the expected signals (Figure 1). A large set of broad signals from 7.20 to 6.20 ppm corresponds to the aromatic protons H_{Ar} of the interlocked crown ether macrocycles DB24C8 (Fig. 1b). The proximity of such protons due to the π-π stacking interactions, as well as the formation of interlocked stereoisomers which accounts for the unsymmetrical substitution of the DB24C8,[50,51] contribute to make this region complicated. However, a slight downfield shift of these protons as well as sharper peaks are observed for the contracted state **9**$_{Cont}$ (Figure 1c), most likely due to the loss of such π-π interactions.

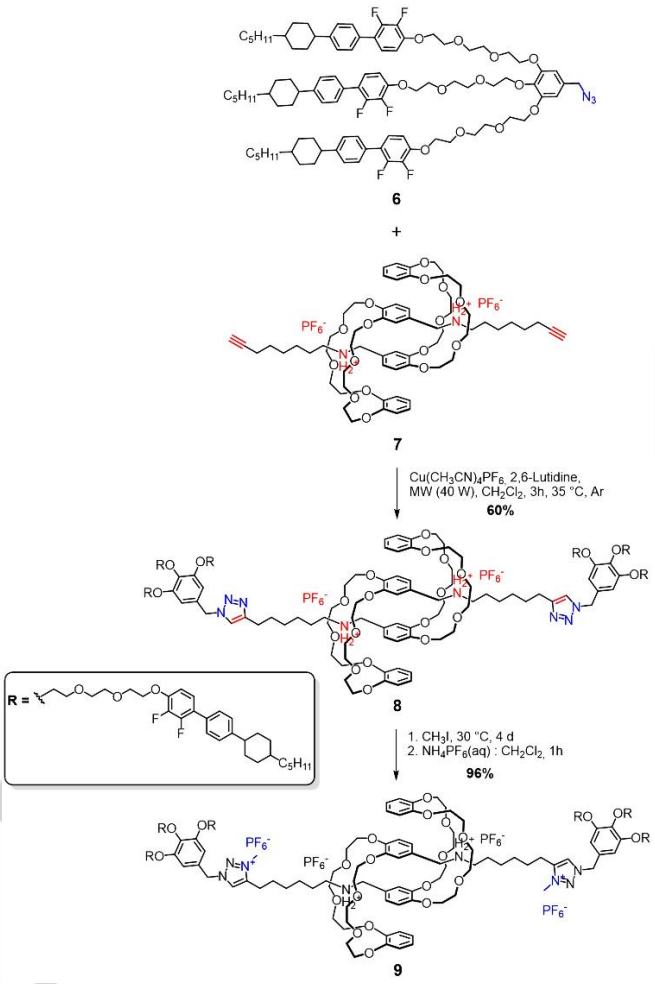

Scheme 2. Synthetic route for [c2]daisy chain rotaxane **9**.

Furthermore, remarkable differences in the chemical shifts of the vinylic proton of the triazolium rings occur between the extended and the contracted states. For **9**$_{Ext}$, proton H_1 (in blue) appears as a singlet at 8.10 ppm. However, upon addition of an aqueous solution of sodium hydroxide, contraction of the molecule occurs leading to a noticeable downfield shift of this signal (9.10 ppm). These observations are in agreement with actuation processes observed for similar [*c*2]daisy chain molecules.[45,52] Interestingly, the signal corresponding to the benzylic protons H_2 (in green) that appears as a singlet at 5.50 ppm in compound **9**$_{Ext}$ moves towards the aromatic region between 6.70 and 6.50 ppm in the contracted state. This particular behaviour suggests that the crown ether macrocycle surrounds the benzylic protons of the gallic moiety, as also supported by the upfield shift of the aliphatic protons H_3 (in pink) adjacent to the triazolium ring (from 2.80 ppm in **9**$_{Ext}$ to 2.40 ppm in **9**$_{Cont}$). Such shift is an indication of the shielding effect exerted by the magnetic field of the aromatic rings, which are sandwiching these protons. An additional shielding effect can be observed for the signal corresponding to CH_3 protons of the triazolium ring (H_4 in orange). This signal appears as a singlet at 4.10 ppm in **9**$_{Ext}$, and is shifted upfield to 3.65 ppm in **9**$_{Cont}$.

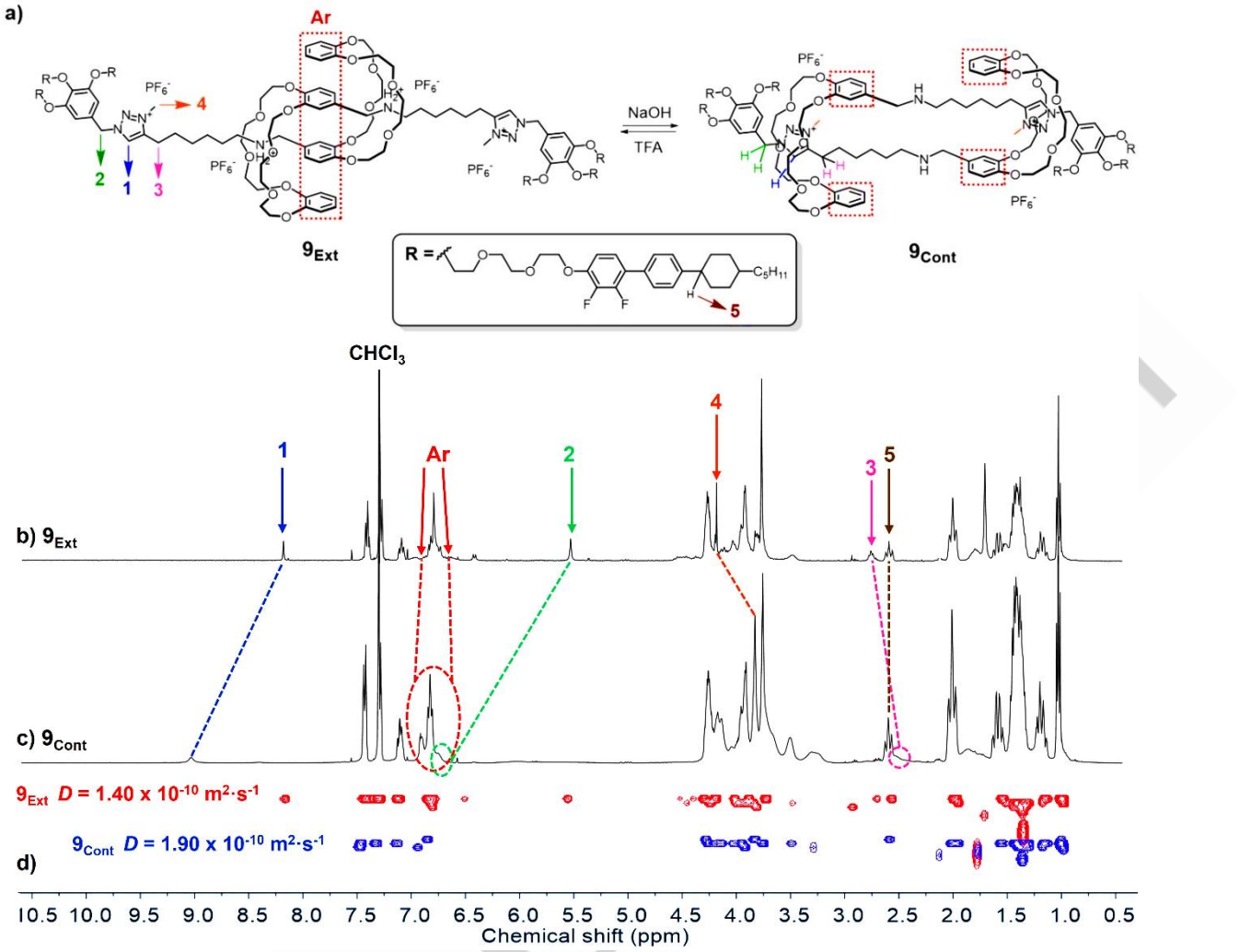

Figure 1. (a) pH-triggered contraction/extension event of [*c*2]daisy chain rotaxane **9**. (b) ^{1}H NMR spectra of $\mathbf{9_{Ext}}$ and (c) $\mathbf{9_{Cont}}$ in $CDCl_3$ and (d) DOSY NMR spectra of $\mathbf{9_{Ext}}$ (red) and $\mathbf{9_{Cont}}$ (blue) recorded in $CDCl_3$ at 26 °C (600 MHz).

Finally, we observe that the proton signals corresponding to the polyether chains and to the alkyl substituents of the mesogen remain very similar whether the molecule is in the contracted or extended state. To confirm the contraction/extension event, we also considered the use of ^{1}H diffusion-ordered spectroscopy (DOSY)[53] to measure the diffusion coefficients of compound **9** in both extended and contracted states. Diffusion NMR experiments were measured on solutions of $\mathbf{9_{Ext}}$ and $\mathbf{9_{Cont}}$ in $CDCl_3$ at 299 K (Figure 1d). For $\mathbf{9_{Ext}}$, the calculated diffusion coefficient (*D*) was *D* = 1.40 x 10^{-10} $m^2 \cdot s^{-1}$, while a higher diffusion coefficient was determined for $\mathbf{9_{Cont}}$ (*D* = 1.90 x 10^{-10} $m^2 \cdot s^{-1}$). These values were used to estimate the hydrodynamic radius of $\mathbf{9_{Ext}}$ (28.0 Å) and $\mathbf{9_{Cont}}$ (20.7 Å) based on the Stokes-Einstein equation,[54] and are consistent with the pH-triggered contraction, since compound $\mathbf{9_{Ext}}$ is 1.4 times larger than $\mathbf{9_{Cont}}$ in solution. On the other hand, the thermal stability of the three interlocked compounds was studied by thermogravimetric analysis (TGA) displaying good thermal stability with decomposition temperatures above 250 °C for **8**, $\mathbf{9_{Ext}}$ and $\mathbf{9_{Cont}}$, (Figure S12).

We subsequently studied the LC properties of $\mathbf{9_{Ext}}$ and $\mathbf{9_{Cont}}$ by experimental techniques including differential scanning calorimetry (DSC) and variable temperature polarised optical microscopy (POM) (Figure 2, S4 and S5). For $\mathbf{9_{Ext}}$, an exotherm between 165 and 175 °C is coherent with a liquid-crystal to isotropic phase transition. For $\mathbf{9_{Ext}}$, upon cooling the sample from the isotropic state, a liquid crystalline texture was observed from ~175 °C (Figure 2b). The phase transition behaviour of compound $\mathbf{9_{Cont}}$ was similar to the one of $\mathbf{9_{Ext}}$, but displaying a shift towards lower temperatures and starting from ~155 °C (Figure 2c and S4). Additionally, shear-induced alignment of the LC texture of the mesophase was observed by POM, confirming the LC behaviour of [*c*2]daisy chain rotaxanes $\mathbf{9_{Ext}}$ and $\mathbf{9_{Cont}}$ down to room temperature (Figure 2d-e). DSC experiments also indicated that no glass transition was detected down to -10°C for both extended and contracted species (Figure S13). One can mention that other systems containing similar dendritic mesogens also exhibit very large LC domains and DSC thermograms with low intensities of the LC-Iso phase transitions.[41,55]

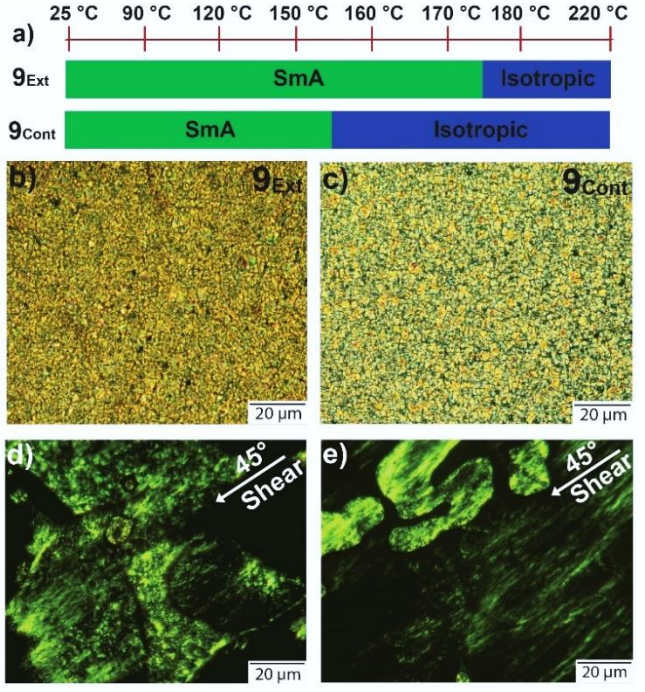

Figure 2 (a) Phase transition behaviours of extended and contracted [*c*2]daisy chain rotaxanes **9**$_{Ext}$ and **9**$_{Cont}$, as determined by DSC experiments. (b-c) Typical POM images of (b) **9**$_{Ext}$ and (c) **9**$_{Cont}$ under crossed polarizer in the LC phase. By cycling the heating and cooling processes 3 times, the measured temperatures of transition did not vary. (d-e) Typical POM images under crossed polarizer of (d) **9**$_{Ext}$ and (e) **9**$_{Cont}$ in the LC phase after shearing at 45°.

To further identify the LC phases, small angle X-ray scattering (SAXS) experiments were carried out on [*c*2]daisy chain rotaxanes in both the extended and contracted states. Both compounds **9**$_{Ext}$ and **9**$_{Cont}$ exhibit in the 0.05 to 0.25 Å^{-1} *q*-range three reflections assigned as (100), (200), and (300) and are characteristic of a SmA mesophase[56] (Figure 3a-b). Importantly, a noticeable change in the interlayer distance was recorded between the extended and contracted daisy chain, in agreement with an actuation of the MIM in the LC phase (Figure 3c-d). Theoretical energy-minimized models of both [*c*2]daisy chain rotaxanes **9**$_{Ext}$ and **9**$_{Cont}$ were computed at the Molecular Mechanics MM2 level (Figure 3e-f). The calculated distance between the ammonium and triazolium stations (approx. 8.0 Å) agrees with the change of the interlayer distance found by SAXS due to the contraction/extension movement triggered by the displacement of the crown ether macrocycle along the axle. The loss of the lamellar packing was also confirmed by SAXS at temperatures above the SmA to isotropic phase transition (Figure S15).

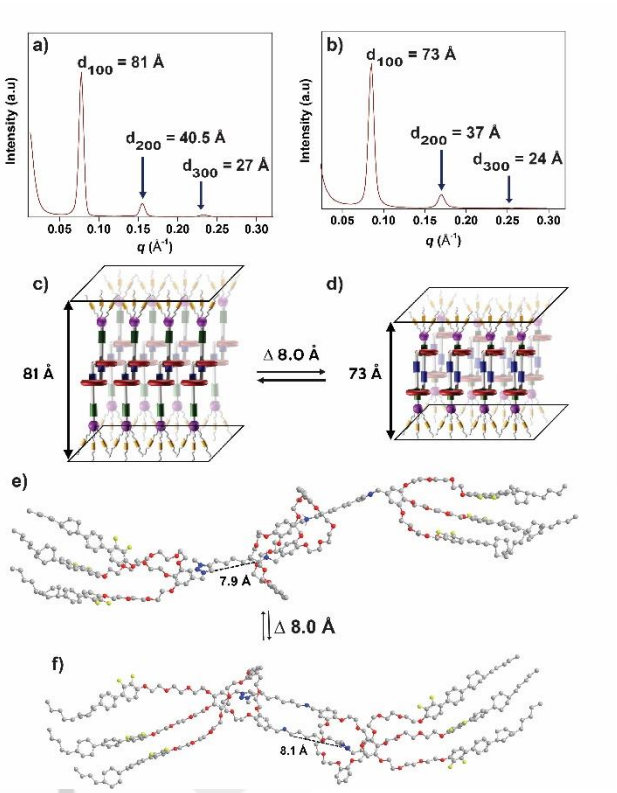

Figure 3. SAXS patterns of **(a)** **9**$_{Ext}$ and **(b)** **9**$_{Cont}$ at 25 °C. (c-d) Schematic representation of the lamellar assembly in the SmA phase of **(c)** **9**$_{Ext}$ and **(d)** **9**$_{Cont}$.(e-f) Molecular modelling of **(e)** **9**$_{Ext}$ and **(f)** **9**$_{Cont}$. The calculated distance between the ammonium and triazolium stations is ≈ 8.0 Å and corresponds to the change of size between the contracted and extended [*c*2]daisy chains . Hydrogen atoms omitted for clarity.

Conclusion

We designed, synthesized, and characterised a pH-responsive bistable [*c*2]daisy chain rotaxane containing two mesogen stoppers. The pH actuation of the bistable interlocked molecule was confirmed by 1D and 2D NMR techniques. The LC phase diagrams of this MIM was characterized by POM micrographs, DSC, and SAXS profiles. It was shown that the extension of the [*c*2]daisy chain results in a ~20 °C decrease of the SmA domain compared to the contracted states. SAXS measurements indicate that this change of the transition temperature is associated to a variation of the characteristic interlamellar distance of the SmA which corresponds to the sliding distance of 8.0 Å within the [*c*2]daisy chain. As a consequence, around 170 °C, the rotaxane can express either a SmA or an isotropic phase depending on its mechanical state. To the best of our knowledge, this work represents the first example of [*c*2]daisy chain architecture with LC properties. It also demonstrates that, at a given temperature, variation of the LC properties can be tuned by the actuation of MIMs, expanding their interest in the field of soft materials science.

Supporting Information

All general methods, synthetic protocols and additional experiments can be found in the Supplementary Information.

Acknowledgements

The authors wish to acknowledge the Fondation Jean-Marie Lehn and the Solvay Company for an excellence doctoral fellowship to C.C.C-V. This work was also supported by the FET-Open project MAGNIFY under grant no. 801378 (fellowship to L.F.) as well as the Japan Society for the Promotion of Science (JSPS, overseas research fellowship to S.T.). We also thank the CARMAC and DiffériX platforms of the Institut Charles Sadron for DSC and SAXS experiments, as well as Dr. Jean-Marc Strub for HRMS experiments.

Keywords: [*c*2]daisy chains • liquid crystals • molecular machines • responsive materials • rotaxanes

[1] J.-P. Sauvage, *Angew. Chem. Int. Ed.* **2017**, *56*, 11080–11093.

[2] J. F. Stoddart, *Angew. Chem. Int. Ed.* **2017**, *56*, 11094–11125.

[3] B. L. Feringa, *Angew. Chem. Int. Ed.* **2017**, *56*, 11060–11078.

[4] V. Balzani, A. Credi, M. Venturi, *Molecular Devices and Machines*, Wiley, **2008**.

[5] S. Erbas-Cakmak, D. A. Leigh, C. T. McTernan, A. L. Nussbaumer, *Chem. Rev.* **2015**, *115*, 10081–10206.

[6] D. Sluysmans, J. F. Stoddart, *Trends Chem.* **2019**, *1*, 185–197.

[7] S. Corra, M. Curcio, M. Baroncini, S. Silvi, A. Credi, *Adv. Mater.* **2020**, *32*, 1906064.

[8] M. Xue, Y. Yang, X. Chi, X. Yan, F. Huang, *Chem. Rev.* **2015**, *115*, 7398–7501.

[9] N. Hoyas Pérez, J. E. M. Lewis, *Org. Biomol. Chem.* **2020**, *18*, 6757–6780.

[10] H. V. Schröder, Y. Zhang, A. J. Link, *Nat. Chem.* **2021**, *13*, 850–857.

[11] M. Denis, S. M. Goldup, *Nat. Rev. Chem.* **2017**, *1*, 0061.

[12] Z. Zhang, W. You, P. Li, J. Zhao, Z. Guo, T. Xu, J. Chen, W. Yu, X. Yan, *J. Am. Chem. Soc.* **2023**, *145*, 567–578.

[13] Q. Zhang, S.-J. Rao, T. Xie, X. Li, T.-Y. Xu, D.-W. Li, D.-H. Qu, Y.-T. Long, H. Tian, *Chem* **2018**, *4*, 2670–2684.

[14] K. Iwaso, Y. Takashima, A. Harada, *Nat. Chem.* **2016**, *8*, 625–632.

[15] E. Moulin, L. Faour, C. C. Carmona-Vargas, N. Giuseppone, *Adv. Mater.* **2020**, *32*, 1906036.

[16] X.-Q. Wang, W.-J. Li, W. Wang, H.-B. Yang, *Acc. Chem. Res.* **2021**, *54*, 4091–4106.

[17] W.-J. Li, W.-T. Xu, X.-Q. Wang, Y. Jiang, Y. Zhu, D.-Y. Zhang, X.-Q. Xu, L.-R. Hu, W. Wang, H.-B. Yang, *J. Am. Chem. Soc.* **2023**, *145*, 14498–14509.

[18] M. C. Jiménez, C. Dietrich-Buchecker, J.-P. Sauvage, *Angew. Chem. Int. Ed.* **2000**, *39*, 3284–3287.

[19] C. A. Henderson, C. G. Gomez, S. M. Novak, L. Mi-Mi, C. C. Gregorio, *Compr. Physiol.* **2017**, *7*, 891–944.

[20] J. Wu, K. C. F. Leung, D. Benítez, J. Y. Han, S. J. Cantrill, L. Fang, J. F. Stoddart, *Angew. Chem. Int. Ed.* **2008**, *47*, 7470–7474.

[21] J. -P. Sauvage, C. Dietrich-Buchecker, Eds. , *Molecular Catenanes, Rotaxanes and Knots*, Wiley, **1999**.

[22] C. J. Bruns, M. Frasconi, J. Iehl, K. J. Hartlieb, S. T. Schneebeli, C. Cheng, S. I. Stupp, J. F. Stoddart, *J. Am. Chem. Soc.* **2014**, *136*, 4714–4723.

[23] W.-J. Li, W. Wang, X.-Q. Wang, M. Li, Y. Ke, R. Yao, J. Wen, G.-Q. Yin, B. Jiang, X. Li, et al., *J. Am. Chem. Soc.* **2020**, *142*, 8473–8482.

[24] S. Tsuda, Y. Aso, T. Kaneda, *Chem. Commun.* **2006**, 3072–3074.

[25] L. Randone, H. Onagi, S. F. Lincoln, C. J. Easton, *Eur. J. Org. Chem.* **2019**, *2019*, 3495–3502.

[26] A. Goujon, E. Moulin, G. Fuks, N. Giuseppone, *CCS Chem.* **2019**, *1*, 83–96.

[27] E. Moulin, C. C. Carmona-Vargas, N. Giuseppone, *Chem. Soc. Rev.* **2023**, DOI: 10.1039/D3CS00619K.

[28] D. Dattler, G. Fuks, J. Heiser, E. Moulin, A. Perrot, X. Yao, N. Giuseppone, *Chem. Rev.* **2020**, *120*, 310–433.

[29] A. Perrot, E. Moulin, N. Giuseppone, *Trends Chem.* **2021**, *3*, 926–942.

[30] L. Chen, X. Sheng, G. Li, F. Huang, *Chem. Soc. Rev.* **2022**, *51*, 7046–7065.

[31] L. F. Hart, J. E. Hertzog, P. M. Rauscher, B. W. Rawe, M. M. Tranquilli, S. J. Rowan, *Nat. Rev. Mater.* **2021**, *6*, 508–530.

[32] A. Goujon, T. Lang, G. Mariani, E. Moulin, G. Fuks, J. Raya, E. Buhler, N. Giuseppone, *J. Am. Chem. Soc.* **2017**, *139*, 14825–14828.

[33] Y. L. Zhao, I. Aprahamian, A. Trabolsi, N. Erina, J. F. Stoddart, *J. Am. Chem. Soc.* **2008**, *130*, 6348–6350.

[34] A. Goujon, G. Mariani, T. Lang, E. Moulin, M. Rawiso, E. Buhler, N. Giuseppone, *J. Am. Chem. Soc.* **2017**, *139*, 4923–4928.

[35] S. Ikejiri, Y. Takashima, M. Osaki, H. Yamaguchi, A. Harada, *J. Am. Chem. Soc.* **2018**, *140*, 17308–17315.

[36] Y. Wang, Q. Li, *Adv. Mater.* **2012**, *24*, 1926–1945.

[37] H. K. Bisoyi, Q. Li, *Chem. Rev.* **2022**, *122*, 4887–4926.

[38] H. K. Bisoyi, Q. Li, *Chem. Rev.* **2016**, *116*, 15089–15166.

[39] J. Sakuda, T. Yasuda, T. Kato, *Isr. J. Chem.* **2012**, *52*, 854–862.

[40] E. D. Baranoff, J. Voignier, T. Yasuda, V. Heitz, J.-P. Sauvage, T. Kato, *Angew. Chem. Int. Ed.* **2007**, *46*, 4680–4683.

[41] I. Aprahamian, T. Yasuda, T. Ikeda, S. Saha, W. R. Dichtel, K. Isoda, T. Kato, J. F. Stoddart, *Angew. Chem. Int. Ed.* **2007**, *46*, 4675–4679.

[42] T. Yasuda, K. Tanabe, T. Tsuji, K. K. Coti, I. Aprahamian, J. F. Stoddart, T. Kato, *Chem. Commun.* **2010**, *46*, 1224.

[43] Y. Abe, H. Okamura, S. Uchida, T. Takata, *Polym. J.* **2014**, *46*, 553–558.

[44] M. Yoshio, T. Mukai, M. Yoshizawa, H. Ohno, T. Kato, *J. Am. Chem. Soc.* **2003**, *125*, 3196–3197.

[45] C. Romuald, E. Busseron, F. Coutrot, *Org. Lett.* **2008**, *10*, 3741–3744.

[46] G. Du, E. Moulin, N. Jouault, E. Buhler, N. Giuseppone, *Angew. Chem. Int. Ed.* **2012**, *51*, 12504–12508.

[47] Y. Wang, C. P. Cabry, M. Xiao, L. Male, S. J. Cowling, D. W. Bruce, J. Shi, W. Zhu, E. Baranoff, *Chem. Eur. J.* **2016**,

22, 1618–1621.

[48] T. M. Kosak, H. A. Conrad, A. L. Korich, R. L. Lord, *Eur. J. Org. Chem.* **2015**, 7460–7467.

[49] A. Goujon, G. Du, E. Moulin, G. Fuks, M. Maaloum, E. Buhler, N. Giuseppone, *Angew. Chem. Int. Ed.* **2016**, *55*, 703–707.

[50] S. J. Cantrill, G. J. Youn, J. F. Stoddart, D. J. Williams, *J. Org. Chem.* **2001**, *66*, 6857–6872.

[51] L. Fang, M. Hmadeh, J. Wu, M. A. Olson, J. M. Spruell, A. Trabolsi, Y. Yang, M. Elhabiri, J. F. Stoddart, *J. Am. Chem. Soc.* **2009**, *131*, 7126–7134.

[52] A. Wolf, J.-J. Cid, E. Moulin, F. Niess, G. Du, A. Goujon, E. Busseron, A. Ruff, S. Ludwigs, N. Giuseppone, *Eur. J. Org. Chem.* **2019**, *2019*, 3421–3432.

[53] C. S. Johnson Jr, *Prog. Nucl. Magn. Reson. Spectrosc.* **1999**, *34*, 203–256.

[54] R. Evans, *Prog. Nucl. Magn. Reson. Spectrosc.* **2020**, *117*, 33–69.

[55] G. Yin, X. Li, H. Peng, H. Yang, *J. Am. Chem. Soc.* **2020**, *142*, 6285–6294.

[56] R. Hou, K. Zhong, Z. Huang, L. Y. Jin, B. Yin, *Tetrahedron* **2011**, *67*, 1238–1244.

Entry for the Table of Contents

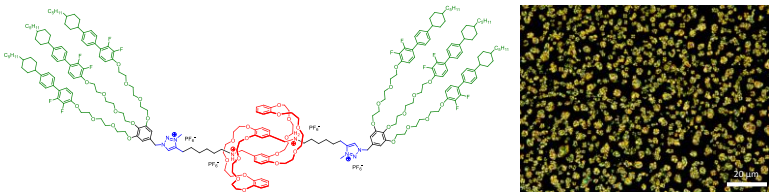

The controlled molecular contraction and extension of a liquid crystalline [c2]daisy chain rotaxane influences its phase diagram behaviour.

Institute and/or researcher Twitter usernames: @GiusepponeLab